Angewandte Chemie
Eine Zeitschrift der Gesellschaft Deutscher Chemiker

Supporting Information

A Polyketide Synthase Component for Oxygen Insertion into Polyketide Backbones

*Roy A. Meoded, Reiko Ueoka, Eric J. N. Helfrich, Katja Jensen, Nancy Magnus, Birgit Piechulla, and Jörn Piel**

anie_201805363_sm_miscellaneous_information.pdf

SUPPORTING INFORMATION

Table of Contents

Experimental Procedures

Phylogenetic analysis of KS domains
All 580 KS sequences from 46 *trans*-AT PKS biosynthetic pathways for which the corresponding metabolite is described in the literature, and two *cis*-AT PKS KS sequences (outgroup) were compiled from our in-house database or retrieved from GenBank. Based on biosynthetic hypotheses as published in a recent review on *trans*-AT PKS biosynthesis [1], updated by recent literature and by manually refinement of biosynthetic models, KS sequences were assigned to a putative substrate. A MUSCLE alignment was generated, manually refined and realigned using the MUSCLE algorithm [2]. MEGA6 [3] was used to generate a maximum likelihood phylogenetic tree, using 100 bootstrap replicates. The LG substitution model, rates and patterns were set to gamma distribution with invariant sites (G+I) and gaps treatment to partial deletion. Parameters for the tree were obtained using the "Find Best Protein Phylogeny" option in MEGA6. Ketide clades were assigned manually and the resulting tree was exported in Newick format and uploaded into iTOL. Graphical representation was conducted in iTOL [4].

Phylogenetic analysis of putative core-PKS Baeyer-Villiger monooxygenases
To analyze the putative core-PKS BVM enzyme family, amino acid sequences of 29 homologs of PedG were retrieved by blast analysis (AAS47561_Symbiont of *Paederus fuscipes*; WP_020915400_*Candidatus* Profftella armatura; AFX60310_*Serratia_marcescens*; AGO55263_*Serratia plymuthica* 4Rx13; WP_012765041_*Dickeya paradisiaca*; WP_016940746_*Dickeya zeae*; WP_024106526_*Dickeya dianthicola*; WP_040001554_*Dickeya chrysanthemi*; WP_022635053_*Dickeya solani*; WP_067221786_*Stappia indica*; WP_008944485_*Oceanibaculum indicum*; WP_055112032_*Labrenzia alba*; WP_069956862_*Magnetovibrio blakemorei*; WP_074768411_*Phaeospirillum fulvum*; WP_024079864_*Magnetospirillum gryphiswaldense*; OJX77727_*Magnetospirillum* sp._64-120; WP_035713094_*Azorhizobium doebereinerae*; WP_026686153_*Azovibrio restrictus*; WP_023131067_*Pseudomonas aeruginosa*; WP_022644435_*Pseudomonas* sp. CMAA1215; WP_081863367_*Azospirillum brasilense*; WP_080682694_*Sorangium cellulosum*; ABK32261_*Sorangium cellulosum*; WP_085317152_*Derxia lacustris*; WP_028311954_*Derxia gummosa*; WP_069094759_*Methyloligella halotolerans*; WP_003598536_*Methylobacterium extorquens*; WP_042129471_*Pseudomonas japonica*; WP_019918768_*Methyloversatilis discipulorum*; WP 018229729_*Methyloversatilis universalis*). The resulting list was supplemented with sequences of representative characterized flavin-dependent enzymes from various sources, including enzymes that had been suggested to catalyze a Baeyer-Villiger reaction and that were discussed in this study [5]. Another phylogenetic tree, containing only PedG-like enzyme sequences and cyclohexanone monooxygenase (AAG10021.1) from *Acinetobacter* sp. SE19 as an outgroup was built. For both trees, the sequences were retrieved from GenBank and aligned using Geneious 7.1.8 using the MUSCLE algorithm and then trimmed. The phylogenetic reconstruction was performed with MEGA6, employing the Maximum Likelihood algorithm with Bootstrap method with 50 replications, LG substitution model with Gamma distributed rates among sites and 5 discrete gamma categories. NNI was chosen as ML heuristic method with branch swap filter set to “very weak” and number of threads set to “1”.

Synthesis of test substrates
***S*-(2-acetamidoethyl) 3-oxoheptanethioate; beta-oxoheptanoyl-SNAC (7)**
The synthesis of **7** was adapted from [6]. A 0 °C solution of the acid chloride (350 mM, 1.0 equiv) in CH_2Cl_2 (8.5 mL) was added to a 0 °C solution of Meldrum’s acid (1.0 equiv, 350 mM) and pyridine (2.0 equiv, 700 mM). The resulting red solution was allowed to react at 0 °C for one hour, then warmed to room temperature for 2 h. The mixture was concentrated under reduced pressure, then dissolved in toluene (200 mM). *N*-acetylcysteamine (1.0 equiv) was added and the red solution was heated to reflux for 2 h under argon. The solution was cooled and quenched with saturated aqueous NH_4Cl (15 mL), extracted with ethyl acetate (2 × 15 mL) and concentrated under reduced pressure. Purification of the residue by silica gel chromatography (SiO_2, 1:1 to 2:8 *n*-hexane/ethyl acetate, 254 nm, R_f (2:8 *n*-hexane/ethyl acetate) 0.38) gave thioester **7** which was recrystallized to afford the desired β-keto thioester (144.6 mg, 22% yield) as a white crystalline solid. The identity was confirmed by ^{1}H NMR (300 MHz, CD_3CN) δ 6.50 (br, 1H), 3.72 (s, 2H), 3.32 – 3.25 (m, 2H), 2.99 (t, J = 6.5 Hz, 2H), 2.52 (t, J = 7.2 Hz, 2H), 1.82 (s, 3H), 1.55-1.45 (m, 2H), 1.35 – 1.23 (m, 2H), 0.89 (t, J=7.15, 3H). Measured ESI-HRMS *m/z* 246.1149 (calculated for $[M+H]^+$ $C_{11}H_{20}NO_3S^+$ 246.1158).

***S*-(2-acetamidoethyl) 3-methylbut-3-enethioate (9)**
Synthesis was performed according to a previously published procedure [7].

***S*-(2-acetamidoethyl) 3-oxobutanethioate (10), *S*-(2-acetamidoethyl) ethanethioate (11),**
Syntheses were performed according to a previously published procedure [8].

***S*-(2-acetamidoethyl) (RS)3-hydroxybutanethioate (12)**
Synthesis was performed according to a previously published procedure [9].

***S*-(2-acetamidoethyl) 4-oxopentanethioate (13)**
Synthesis was performed according to a previously published procedure [10].

***S*-(2-Acetamidoethyl) 2-phenylethanethioate (14), *S*-(2-Acetamidoethyl) (*E*)-3-phenylprop-2-enethioate (15)**
Syntheses were performed according to a previously published procedure [11].

***S*-(2-acetamidoethyl) octanethioate (16), *S*-(2-acetamidoethyl) 3-methylbut-3-enethioate (17), *S*-(2-acetamidoethyl) 3-oxododecanethioate (8)**
Syntheses were performed according to a previously published procedure [12].

SUPPORTING INFORMATION

Construction of the *oocK*, *pedG*, and *tobD* expression plasmids

The *oocK* gene was amplified from a *Serratia plymuthica* 4Rx13 colony using the primer pair *oocKNco*I_F and *oocKBgl*II_R. The gel-purified gene fragment was digested with *Nco*I and *Bgl*II and cloned into pBAD/*Myc*-His A, yielding the plasmid pBAD*oocK*. The plasmid was modified by amplification with the primers pBAD*oocKNde*IQC_F and pBAD*oocKNde*IQC_R, yielding pBAD*oocK*QC. The plasmid was isolated and introduced into *E. coli* DH5α as well as *S. plymuthica* 4Rx13Δ*oocK*. pBAD*oocK*QC was then used as a template for amplification of *oocK* using primers pBAD*oocKNde*IQC_F and *oocK*N'*Not*I_R. The gel-purified gene fragment was digested with *Nde*I and *Not*I and cloned into pET28-derived vector with a modified tag region for C-terminal fusion, namely pET28HB-TS, yielding pET28HB-TS*oocK*. Only the N-terminal variant was used in this study. The plasmid was isolated and introduced into *E: coli* Tuner™ (DE3) competent cells (Novagen). This strain was used for the expression of N-terminally His_6-tagged OocK.

The *pedG* gene was amplified from the cosmid pPD9F12, harboring part of the pederin biosynthetic gene cluster [13] using the primer pair *pedGPci*I_F and *pedGHind*III_*R*. The gel-purified gene fragment was digested with *Pci*I and *Hind*III and cloned into pBAD/*Myc*-His A, yielding the plasmid pBAD*pedG*. The plasmid was modified by amplification with the primers pBAD*pedGNde*IQC_F and pBAD*pedGNde*IQC_R, yielding pBAD*pedG*QC while introducing the *Nde*I restriction site at the 5'end of the gene. The plasmid was isolated and introduced into *E. coli* DH5α. pBAD*oocK*QC was then subcloned into pET28HB-TS using the restriction sites *Nde*I and *Hind*III, yielding pET28HB-TS*pedG*. The plasmid was isolated and introduced into *E. coli* Tuner™ (DE3) competent cells (Novagen). This strain was tested for the expression of N-terminally His_6-tagged PedG.

The *tobD* gene was amplified from a fresh culture of *Methylobacterium extorquens* AM1 using the primer pair *tobDNco*I_F and *tobDHind*III_R. The gel-purified gene fragment was digested with *Nco*I and *Hind*III and cloned into pBAD/*Myc*-His A, yielding the plasmid pBAD*tobD*. The plasmid was modified by amplification with the primers pBAD*tobDNde*IQC_F and pBAD*tobDNde*IQC_R, yielding pBAD*tobD*QC while introducing the *Nde*I restriction site at the 5'end of the gene. The plasmid was isolated and introduced into *E. coli* DH5α. pBAD*tobD*QC was then subcloned into pET28HB-TS using the restriction sites *Nde*I and *Hind*III, yielding pET28HB-TS*tobD*. The plasmid was isolated and introduced into Tuner™ (DE3) competent cells (Novagen). This strain was tested for the expression of N-terminally His_6-tagged TobD.

Generation of *S. plymuthica* 4X13Δ*oocK*

The knockout strain *S. plymuthica* 4X13Δ*oocK* was generated as described in [14] with the primers KO_SOD_b00960_fwd and KO_SOD_b00960_rev.

Complementation experiment with OocK

For complementation experiments, *S. plymuthica* 4X13Δ*oocK* cells were introduced by electroporation with either an empty pBAD/*Myc*-His-A or pBAD*oocK*. Cultures of *S. plymuthica* 4Rx13 WT, *S. plymuthica* 4X13Δ*oocK*, *S. plymuthica* 4X13Δ*oocK* harboring an empty pBAD/*Myc*-His-A and *S. plymuthica* 4X13Δ*oocK* harboring pBADΔ*oocK* were inoculated from overnight cultures (1/100) and grown in 20 mL of EPB medium (250 rpm, 26 °C). Cultures with *S. plymuthica* 4Rx13 harboring either the empty pBAD/*Myc*-His-A or pBAD*oocK* were supplemented with 100 µg/mL carbenicillin and also induced with 0.2% arabinose after 16 h. The cultures were extracted with ethyl acetate after 24 h, and concentrated under reduced pressure. Extracts were resuspended in methanol and subjected to data-dependent ultra-high performance liquid chromatography-high resolution heated electrospray-tandem mass spectrometry (UHPLC HR HESI MS^2) analysis using a Dionex Ultimate 3000 UPLC system connected to a Thermo QExactive mass spectrometer. A solvent gradient (A = H_2O + 0.1% formic acid and B = acetonitrile + 0.1% formic acid with B at 5% for 0-2 min, 5-50% for 2-4 min, 50-95% for 4-10 min, and 95% for 10-13 min at a flow rate of 1.0 mL/min) was used on a Phenomenex Kinetex 2.6 µM C18 100A (150 × 4.6 mm) column at 27 °C. The MS was operated in positive ionization mode at a scan range of 150-1500 *m/z* to account for single charged oocydins. The spray voltage was set to 3.7 kV and the capillary temperature to 320 °C. MS^2 data were acquired in a data-dependent fashion with the parent ion scan at a resolution of 70,000 and the MS^2 scan at a resolution of 17,500. The ten most abundant peaks of each parent ion scan were subjected to CID fragmentation with a normalized collision energy (NCE) of 15, 25 and 35 for network analysis and the dynamic exclusion time was set to 10 sec. MS^2 scans were conducted with an AGC target of 3×10^6 or a maximum injection time of 150 ms. Thermo raw files were converted into mzXML file format using MSExport, and uploaded onto the GNPS web server [15]. For network analysis, the data were filtered by removing all MS^2 peaks within +/- 17 Da of the precursor *m/z*. MS^2 spectra were window-filtered by choosing only the top 6 peaks in the +/- 50 Da window throughout the spectrum. The data were then clustered with MS-Cluster with a parent mass tolerance of 0.2 Da (to minimize isotopes of halogenated oocydins appearing as different nodes in the network) and a MS^2 fragment ion tolerance of 0.2 Da to create consensus spectra. Further, consensus spectra that contained less than 2 spectra were discarded. A network was then created where edges were filtered to have a cosine score above 0.7 with at least six matched peaks. Edges between two nodes were kept in the network if each of the nodes appeared in each other's respective top ten most similar nodes (18). Data were downloaded and visualized using Cytoscape 3.2 [16].

Heterologous gene expression and protein purification of OocK

The *E. coli* expression strains were grown in TB medium supplemented with 50 µg/mL kanamycin until an optical density (OD) of 0.4-0.6 was reached, after which the culture was cooled on ice for 15 min. Gene overexpression was induced by addition of isopropyl β-D-1-thiogalactopyranoside (IPTG) to a concentration of 0.1 mM. Induced cultures were grown for additional 16-20 h at 16 °C and afterwards harvested by centrifugation. Cell pellets were either processed directly or frozen and stored at -80 °C. All purification steps were carried out at 4 °C. Cells were resuspended in lysis buffer (50 mM phosphate buffer pH 8.0, 300 mM NaCl, 20 mM imidazole, 10% [v/v] glycerol) and disrupted by sonication using a Sonicator Q700 (QSonica, Newton, USA). The lysate was centrifuged for 20 min at 18,000 g to remove cell debris. The supernatant was incubated with Ni-NTA agarose (Macherey-Nagel, Oensingen, Switzerland) for 15 min and transferred to a fretted column. The resin was washed once with 5 mL lysis buffer and finally eluted twice with 0.75 mL elution buffer (50 mM phosphate buffer pH 8.0, 300 mM NaCl, 250 mM imidazole, 10% glycerol). Yellow elution fractions were verified to contain the eluted protein by SDS-PAGE.

Biochemical assays

Purified OocK was separately incubated with SNACs (**7-17**) to mimic naturally occurring ACP-tethered polyketide intermediates. These included the predicted substrates β-keto substrates (**7-10)**, as well other, structurally diverse SNACs (**11-17**). All substrates were weighed in and individually dissolved in DMSO to a stock concentration of 80 mM. The assay was set up in a volume of 100 µL, containing 2-5 µM of OocK, 200 µM of the SNAC substrate (from 80 mM stock in DMSO), 200 µM NADPH, 10% [v/v] glycerol and 50 mM phosphate buffer pH 7.0. Negative controls included OocK enzyme that was boiled at 98 °C for 10 min prior to addition of the

substrates and NADPH. Reactions were incubated at room temperature for 90 min, extracted with ethyl acetate, dried, and redissolved in 200 µL methanol and subsequently analyzed by LC-MS. Measurements were conducted on a QExactive Orbitrap MS (Thermo Scientific, Reinach, Switzerland) coupled to an UltiMate 3000 UHPLC system (Dionex, Reinach, Switzerland).
A solvent gradient (A = H_2O + 0.1% formic acid and B = acetonitrile + 0.1% formic acid was used on a Kinetex 2.6 µm C8 100 Å, LC Column (150 × 4.6 mm; Phenomenex, Torrance, CA, USA). In Fig. S6 the gradient was solvent B at 5% for 0-2 min, 5-50% for 2-4 min, 50-70% for 4-7 min and 95% for 7-9 min at a flow rate of 1.0 mL/min. In Fig. 4 the gradient was solvent B at 5% for 0-3 min, 5-25% for 3-5 min, 25% for 5-25 min, 25-95% for 25-26 min, 95% for 26-32 min at a flow rate of 1.0 mL/min. MS measurement was conducted in positive ionization mode in a mass range of 100 - 1000 *m/z*. Collected data of all MS experiments was analyzed using the Thermo Xcalibur 2.2. software.
For NMR analysis, the reaction was scaled up to 10 mL. The product was purified by reversed-phase HPLC (Phenomenex, Luna C8, 100 Å, 5 u, 250 x 10.00 mm) with an isocratic flow of 2 mL/min 25% solvent B. The dried product was then resuspended in CD_3CN.

Size exclusion chromatography
OocK solution or a calibration mixture of three proteins; Aldolase (158 kDa), Conalbumin (75 kDa) and Ribonuclease A (13.7 kDa) were loaded on a GE Healthcare Superdex Increase 10/300 column and analyzed with an isocratic flow of 0.5 mL/min of 50 mM PBS buffer pH 7.7, 300 mM NaCl at 4 °C for 50 min.

Isolation of oocydin B (31) from *S. plymuthica* 4Rx13
S. plymuthica 4Rx13 was cultured with XAD 16N. The supernatant was decanted, and the resin washed with dH_2O (10 mL/L culture) and extracted with methanol (15 mL/L culture). The extract was stirred for 30 min at room temperature and the organic layer dried under reduced pressure. After treating the residue with water, the mixture was extracted with chloroform. The aqueous layer was re-extracted with ethyl acetate and the combined organic layers dried under reduced pressure. The extract was subjected to HPLC purification. A solvent gradient (A = H_2O + 0.1% TFA and B = acetonitrile + 0.1% TFA acid with B at 35% for 0-60 min, 35-95% for 60-70 min at a flow rate of 15.0 mL/min) was used on a Phenomenex, Luna, C18(2), 100 Å, 5 u, 250 x 21.20 (detection: 210 nm). The fractions between 70-73 minutes were collected and the solvent was removed under reduced pressure. The dried fractions were subjected to a second round of HPLC purification. A solvent gradient (A = H_2O + 0.1% TFA and B = acetonitrile + 0.1% TFA with B at 60% for 0-60 min, 60-100% for 60-70 min and 95% for 10 min at a flow rate of 2 mL/min) on a Phenomenex, Luna Phenyl-Hexyl, 100 Å, 5 u, 250 x 10.00 (detection: 210 nm). The solvent was removed under reduced pressure, yielding 0.5 mg of pure compound that was subjected to NMR measurements.

Structure elucidation of 18 and 31
NMR spectra were recorded on a Bruker Avance III spectrometer equipped with a cold probe at 600 MHz for ^{1}H NMR and 150 MHz for ^{13}C NMR. Chemical shifts were referenced to the solvent peak at δ_H 7.27 and δ_C 77.2 for chloroform-*d*, δ_H 3.31 and δ_C 49.2 for methanol-d_4, and δ_H 1.94 and δ_C 1.3 for acetonitrile-d_3.

SUPPORTING INFORMATION

Results and Discussion

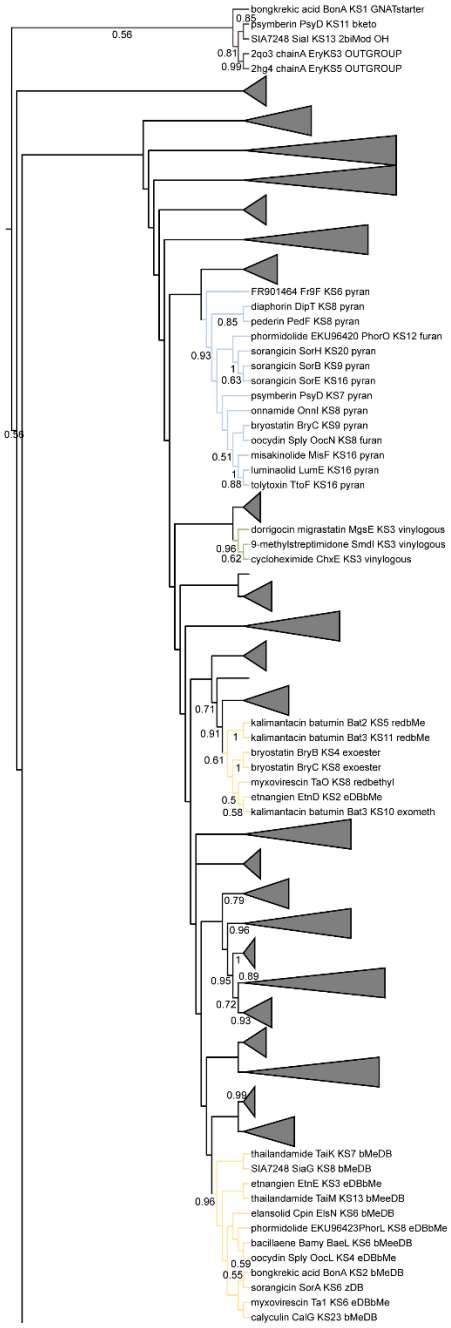

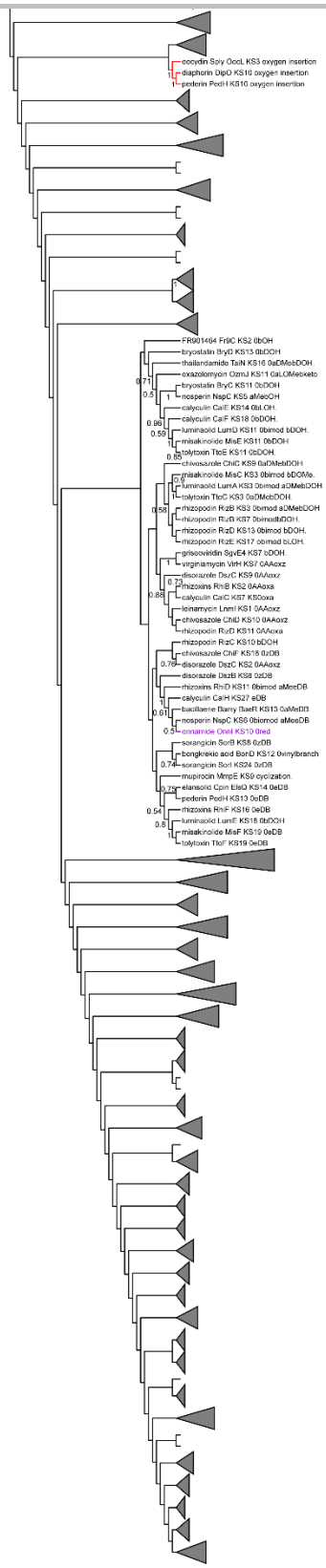

Figure S1. Phylogram of 580 *trans*-AT PKS KS domains and distinct biochemical transformations encountered in *trans*-AT PKS systems. A maximum likelihood phylogenetic tree was inferred for *trans*-AT PKS KS sequences from *trans*-AT PKS BGCs for which the corresponding metabolite has been identified. *Cis*-AT PKS KS domains from the erythromycin PKS were used as outgroup (top). Grey indicates canonical ketide clades. Bootstrap values higher than 0.5 are indicated. Ketide clades that correspond to oxygen insertion, β-branching, vinylogous chain branching, and pyran ring formation are expanded to indicate bootstrap values and members of a ketide clade.

SUPPORTING INFORMATION

Ketide clade nomenclature: polyketide name_protein_location of KS (number of the KS starting from the first KS of the pathway according to published biosynthetic models)_substrate specificity (see Fig. 2). The pederin (*ped*) and onnamide (*onn*) PKSs diverge after KS9. In the case of pederin, the subsequent KS (pedKS10) putatively recognizes oxygen insertion events and in the case of onnamide the subsequent KS is the non-elongating onnKS10 (purple).

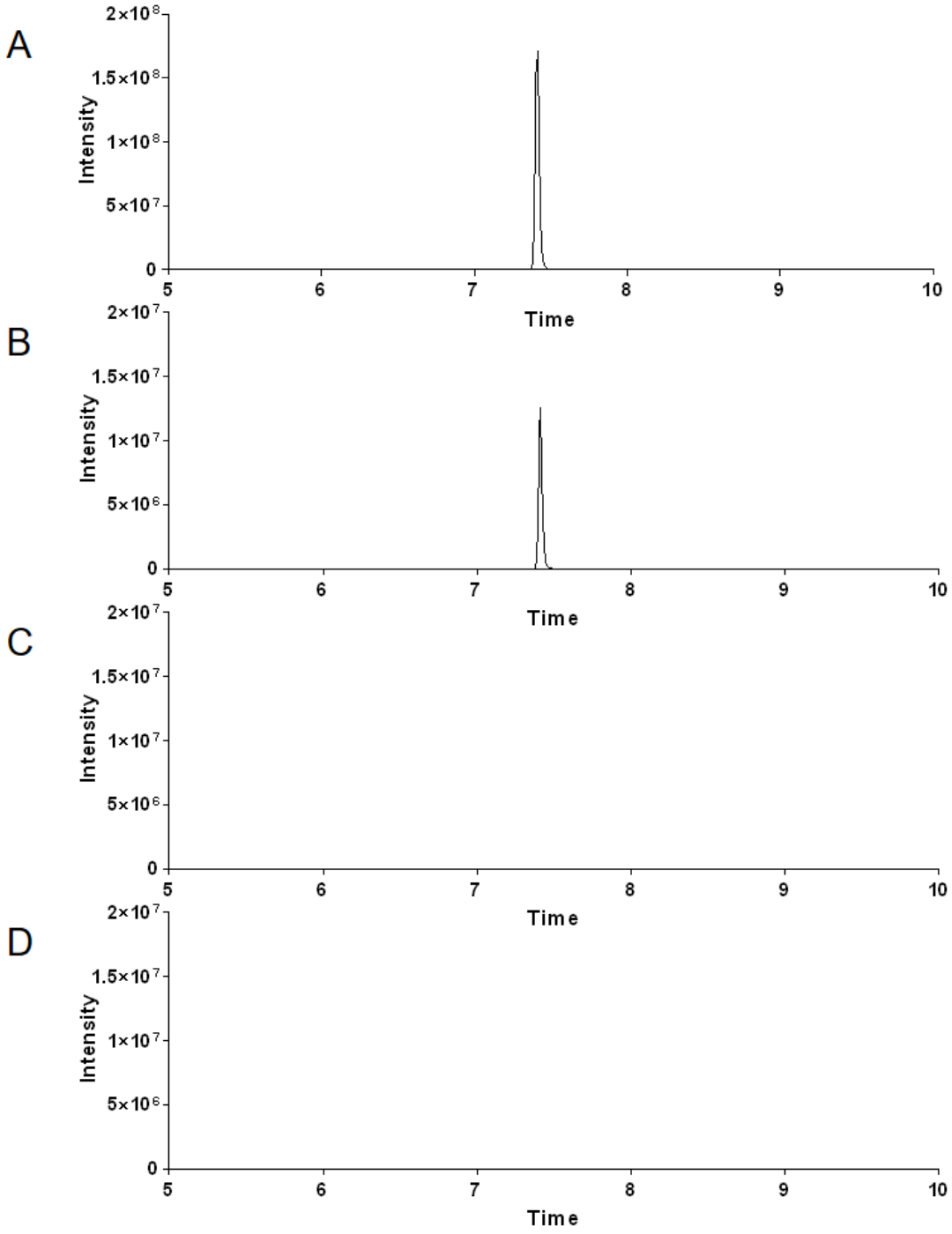

Figure S2. Extracted ion chromatogram (EIC) for oocycin A (calculated for $[M+NH_4]^+$ $C_{23}H_{35}NClO_8^+$ 488.2046 from *S. plymuthica* 4Rx13 wild-type (WT) and mutant strains (*A*) WT. (*B*) *S. plymuthica* 4Rx13Δ*oocK* complemented with pBAD*oocK*. (*C*) *S. plymuthica* 4Rx13Δ*oocK* complemented with an empty pBAD vector. (*D*) *S. plymuthica* 4Rx13Δ*oocK*. Notice that the scale of chromatogram A is an order of magnitude higher than chromatograms B-D.

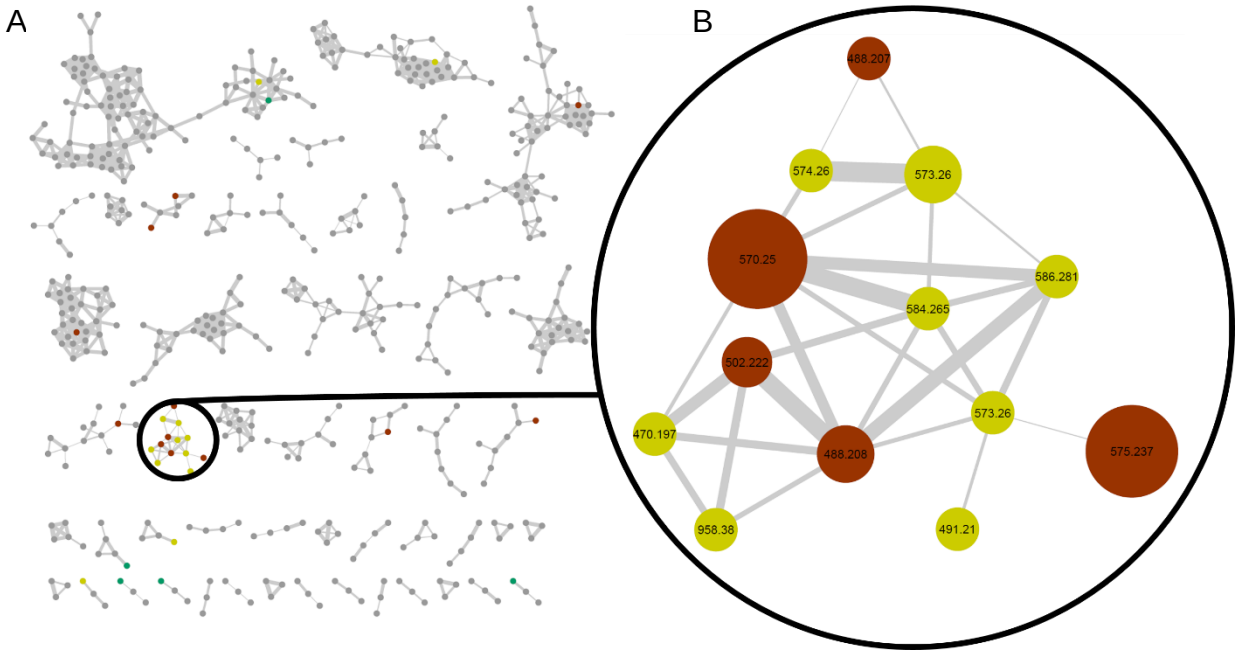

Figure S3. Molecular network analysis of oocydins. Nodes are color-coded according to the *S. plymuthica* 4Rx13 strains from which the data were obtained: yellow; WT, green; Δ*oocK* harboring pBAD*oocK*, red; metabolites present in both samples, grey; Δ*oocK* and/or Δ*oocK* harboring an empty pBAD vector. Node labels indicate the parent mass. This figure represents only singly-charged parent ions. (*A*) Molecular network analysis of all clusters harboring more than two nodes. The relevant cluster containing the oocydin congener parent masses is framed in black. (*B*) Enlarged view of the cluster showing parent masses corresponding to oocydin congeners. The node size reflects the parent mass intensity for each metabolite as a proxy for their relative abundance. The edge line width indicates the relatedness between two metabolites (cosine 0.7).

A

B

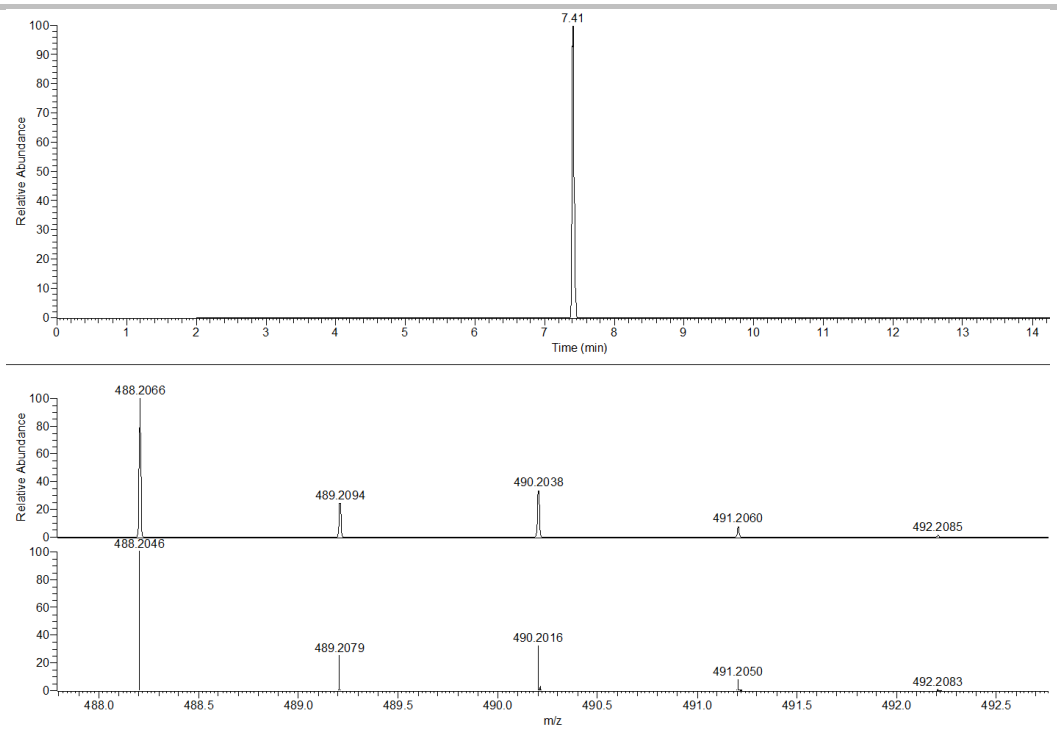

Figure S4. UHPLC-HRMS data of oocydin A (**4**). (*A*) EIC of oocydin A (**4**). (*B*) Mass spectrum of oocydin A (**4**, upper), showing characteristic isotopic pattern as compared with a simulated mass spectrum for the molecular formula of the ammonium adduct of oocydin A (**4**, lower).

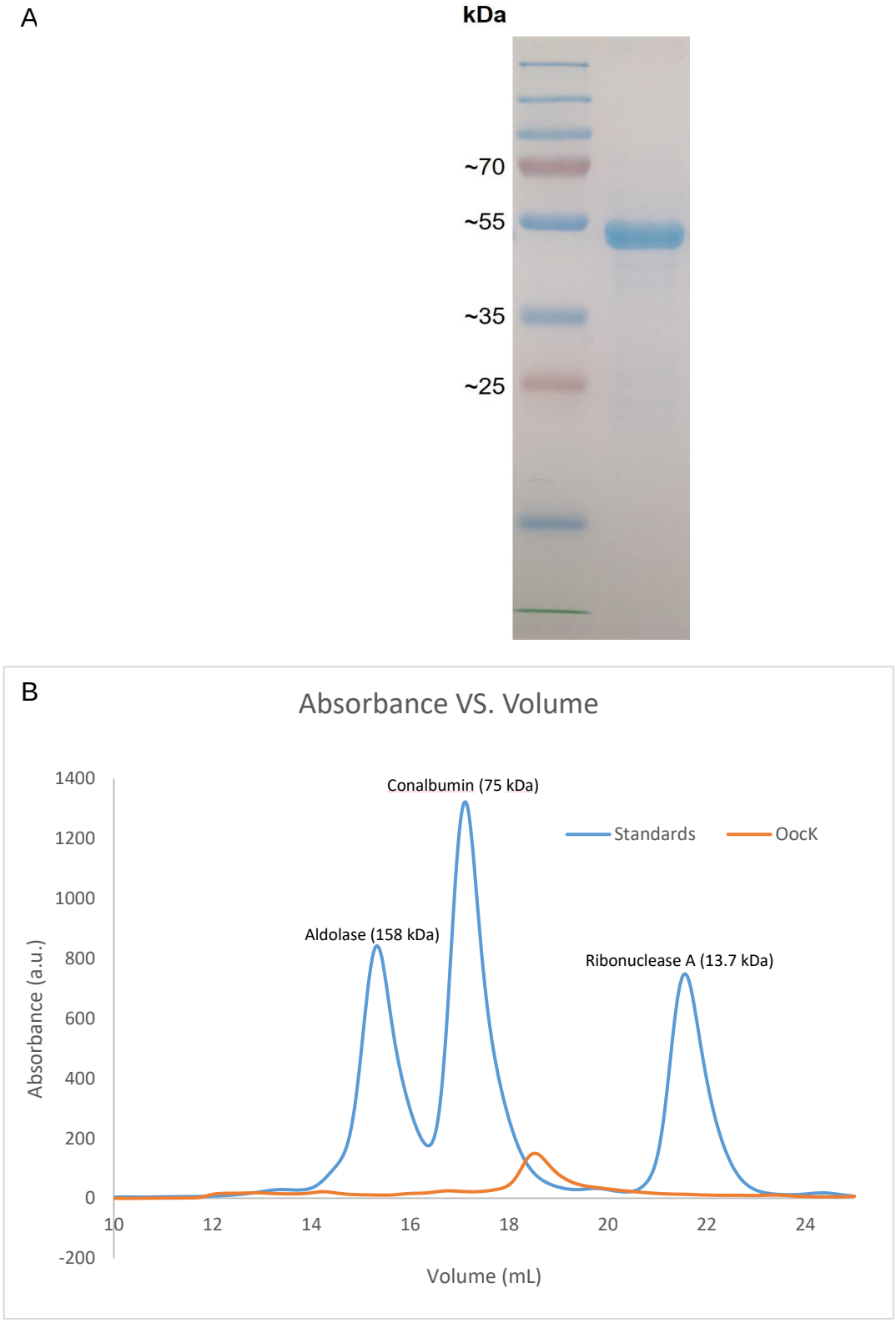

Figure S5. Characterization of OocK. (*A*) 12% SDS-PAGE gel of OocK (expected molecular weight: 52.0 kDa) post His_6-tag purification. (*B*) Size exclusion chromatography of OocK in comparison with the proteins Aldolase (158 kDa), Conalbumin (75 kDa) and Ribonuclease A (13.7 kDa), suggesting that OocK assumes a monomeric state in the conditions tested, without PKS protein partners.

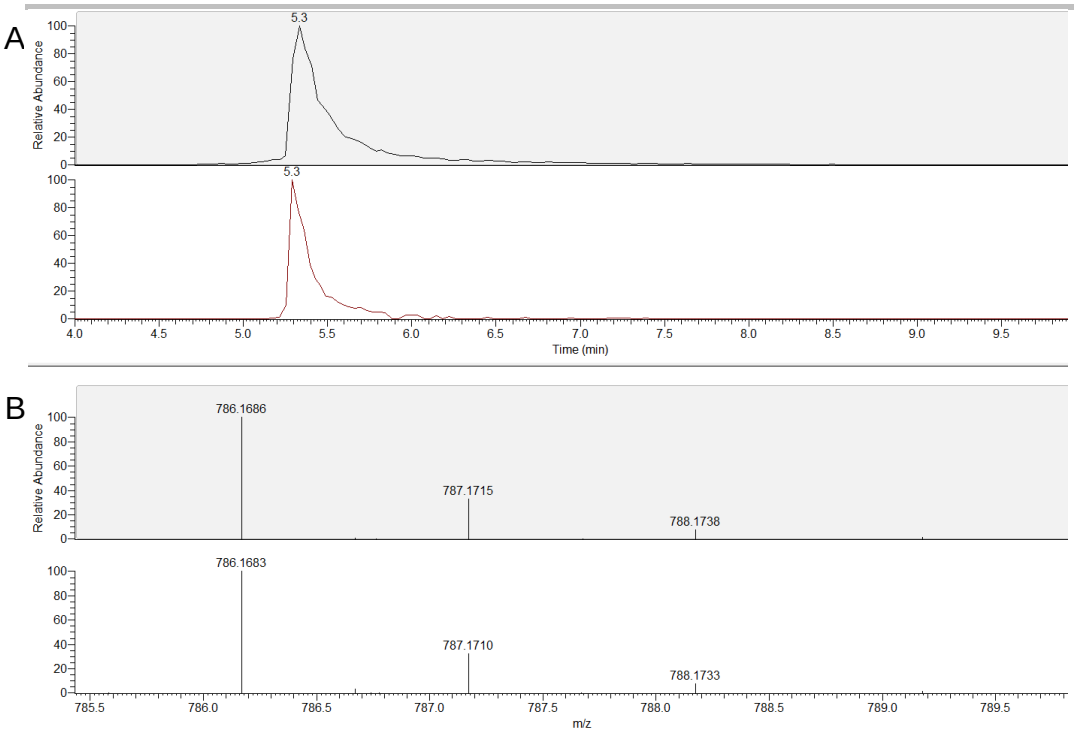

Figure S6. UHPLC-HRMS data for the FAD analysis. (*A*) EIC of FAD extracted from purified OocK (upper) and of the FAD standard (lower). (*B*) Mass spectrum of FAD extracted from purified OocK (upper) and of the FAD standard (lower).

SUPPORTING INFORMATION

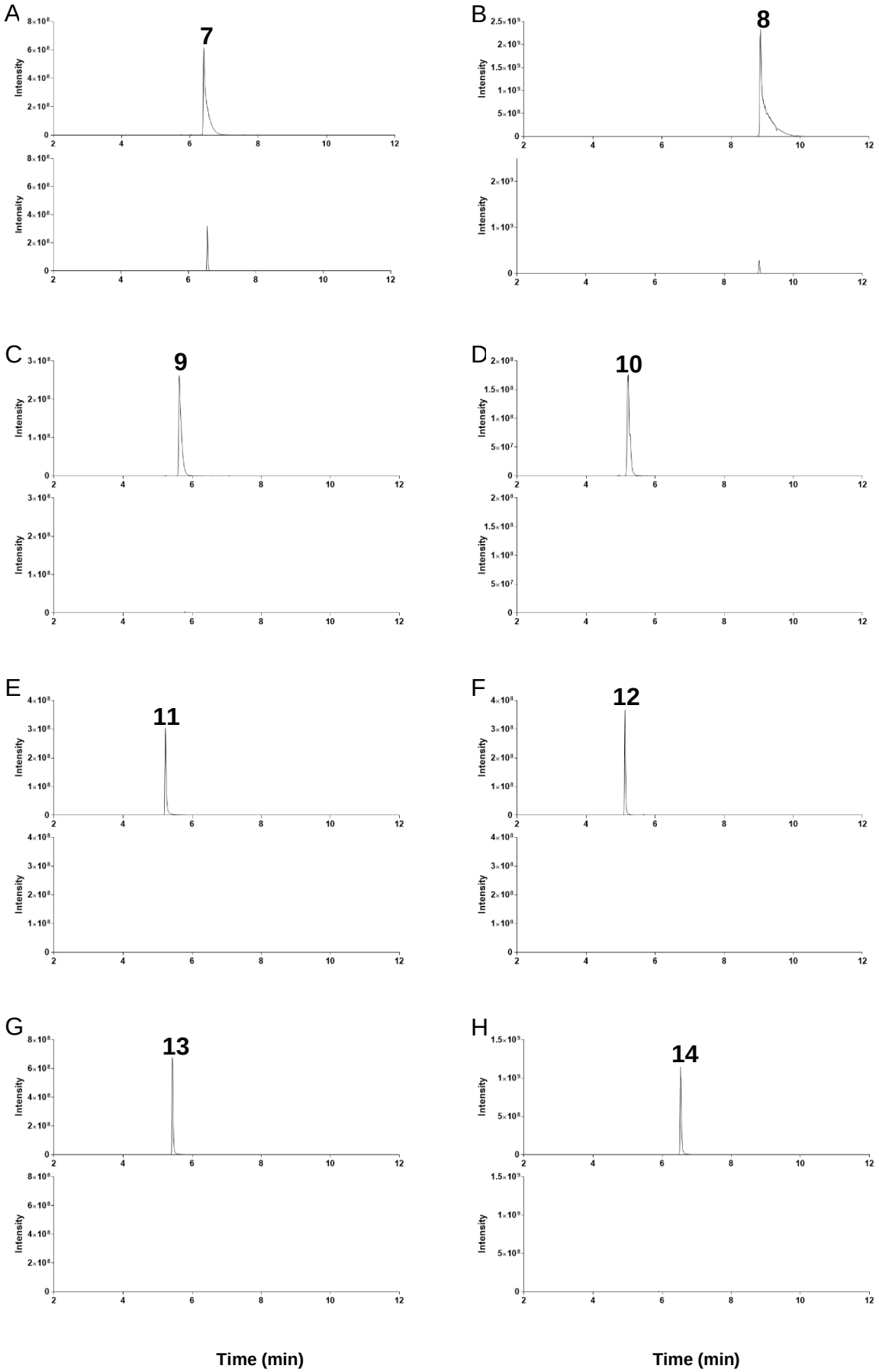

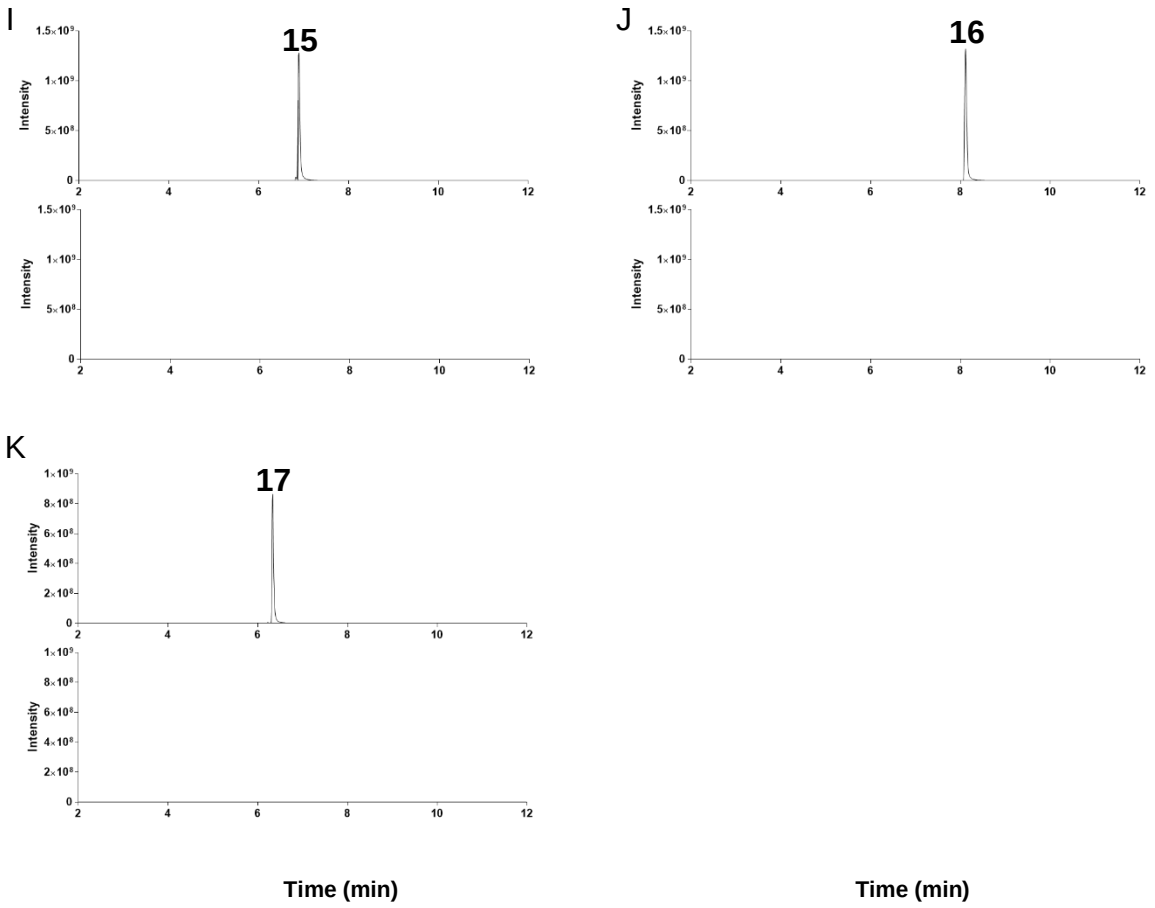

Figure S7. UHPLC-HRMS data for the analysis of the enzymatic assays with OocK and various potential substrates, displaying in each panel the EIC calculated for the substrate as $[M+H]^+$ (upper) and the putative product as $[M+^{16}O+H]^+$ (lower). Putative product peak formation was only detectable for assays with OocK incubated with **7** and **8**. (*A*) Assay with **7** (EIC: *m/z* 246.1158 and *m/z* 262.1108). (*B*) Assay with **8** (EIC: *m/z* 316.1941 and *m/z* 332.1890). (*C*) Assay with **9** (EIC: *m/z* 218.0845 and *m/z* 234.0795). (*D*) Assay with **10** (EIC: *m/z* 204.0689 and *m/z* 220.0638). (*E*) Assay with **11** (EIC: *m/z* 162.0583 and *m/z* 178.0532). (*F*) Assay with **12** (EIC: *m/z* 206.0845 and *m/z* 222.0795). (*G*) Assay with **13** (EIC: *m/z* 218.0845 and *m/z* 234.0795). (*H*) Assay with **14** (EIC: *m/z* 238.0896 and *m/z* 254.0845). (*I*) Assay with **15** (EIC: *m/z* 250.0896 and *m/z* 266.0845). (*J*) Assay with **16** (EIC: *m/z* 246.1522 and *m/z* 262.1471). (*K*) Assay with **17** (EIC: *m/z* 202.0896 and *m/z* 218.0845).

A

B

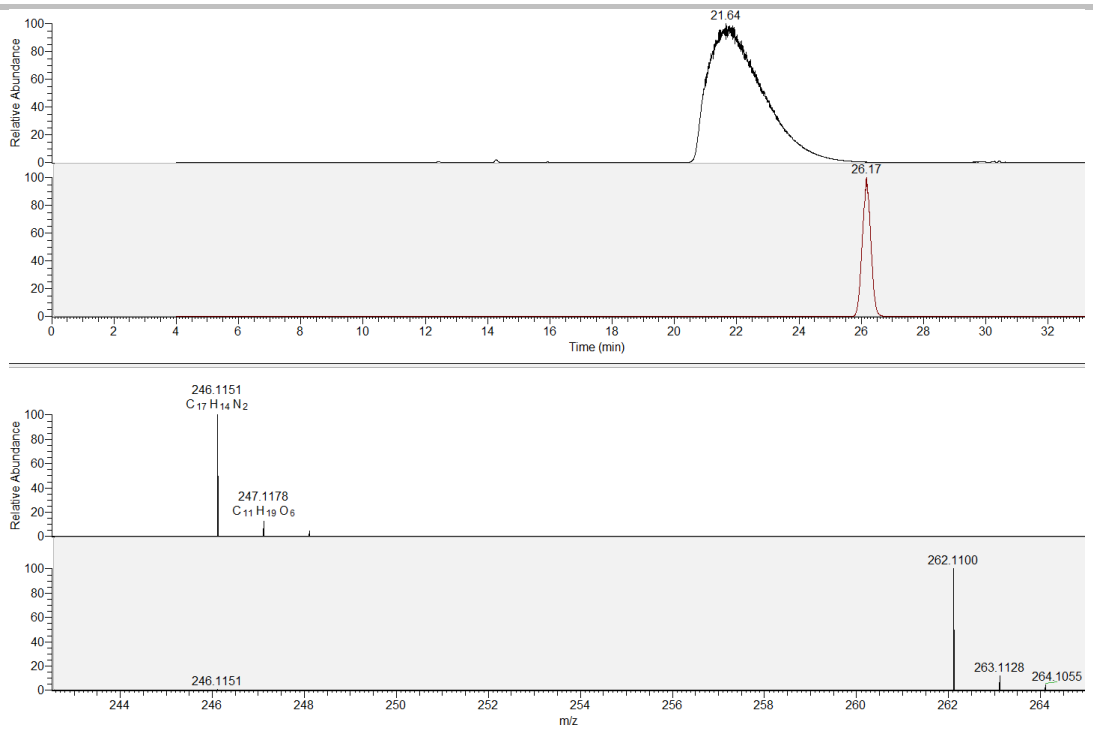

Figure S8. UHPLC-HRMS data of the enzymatic assay of OocK with **7**. **(***A*) EIC of the assay substrate **7** (upper) and product **18** (lower). (*B*) Mass spectrum of **7** (upper) and of product **18** (lower).

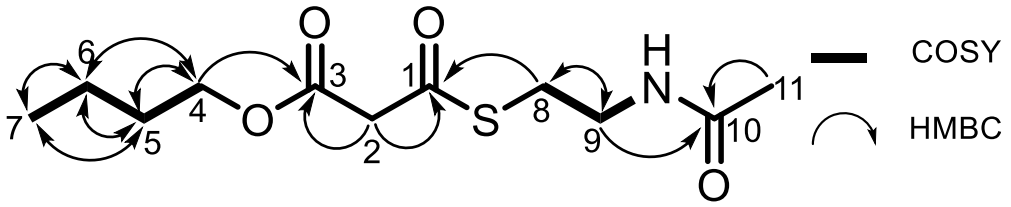

Figure S9: COSY and HMBC correlations of **18**.

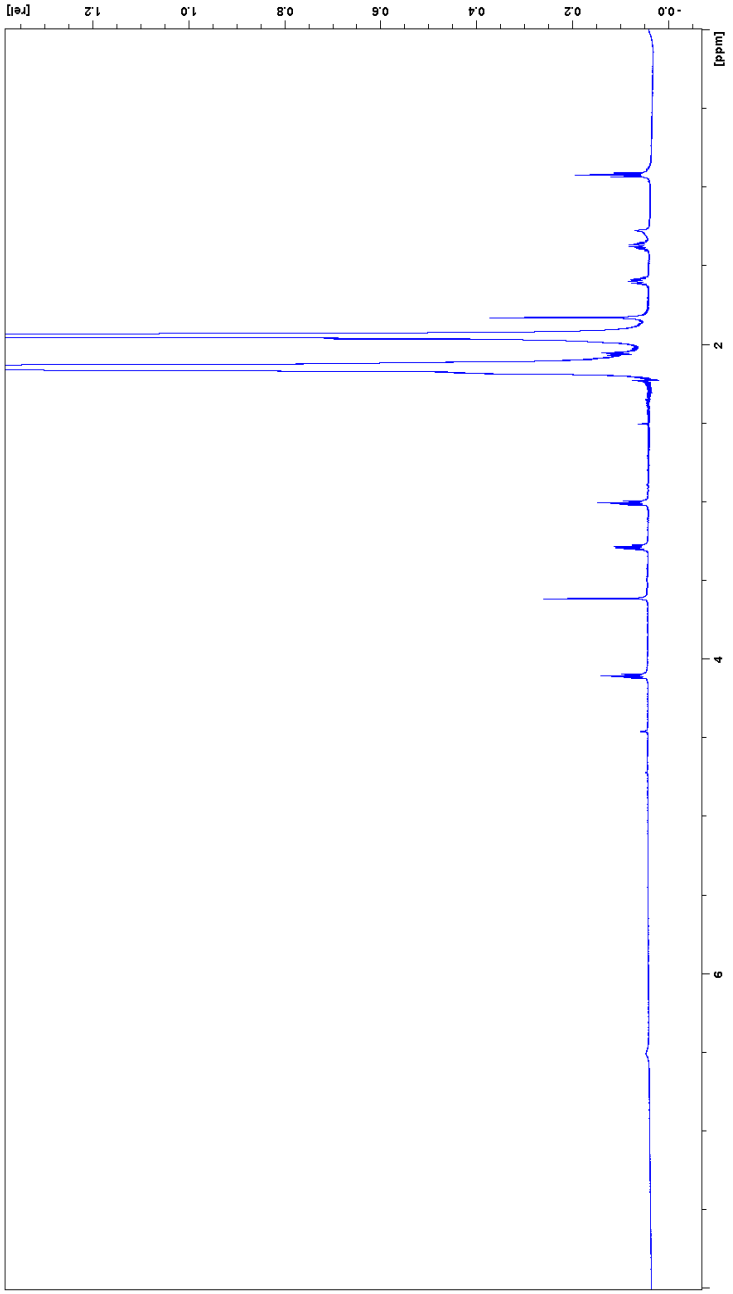

Figure S10: ^{1}H NMR spectrum of **18** in acetonitrile-d_3 at 600 MHz.

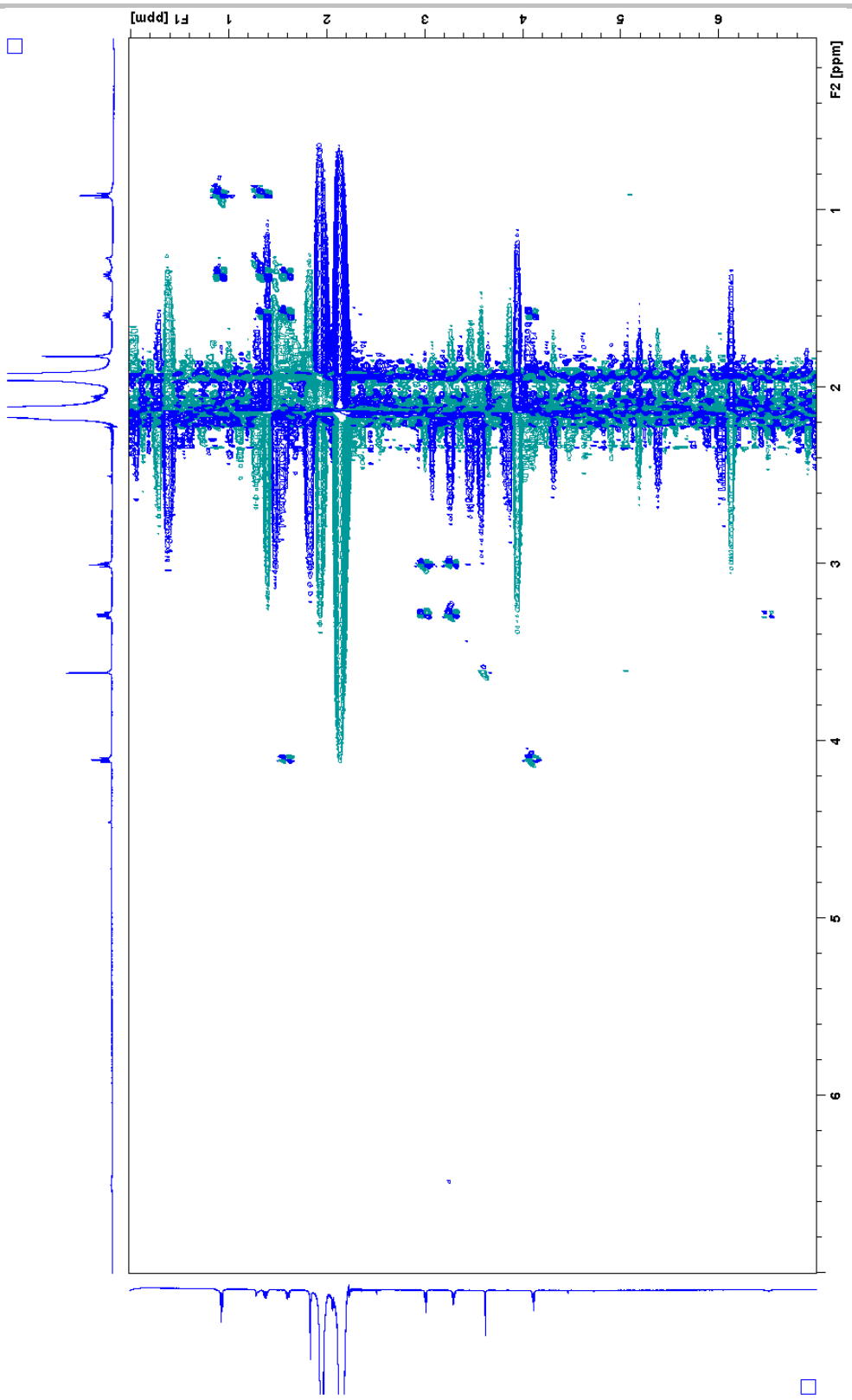

Figure S11: COSY spectrum of **18** in acetonitrile-d_3.

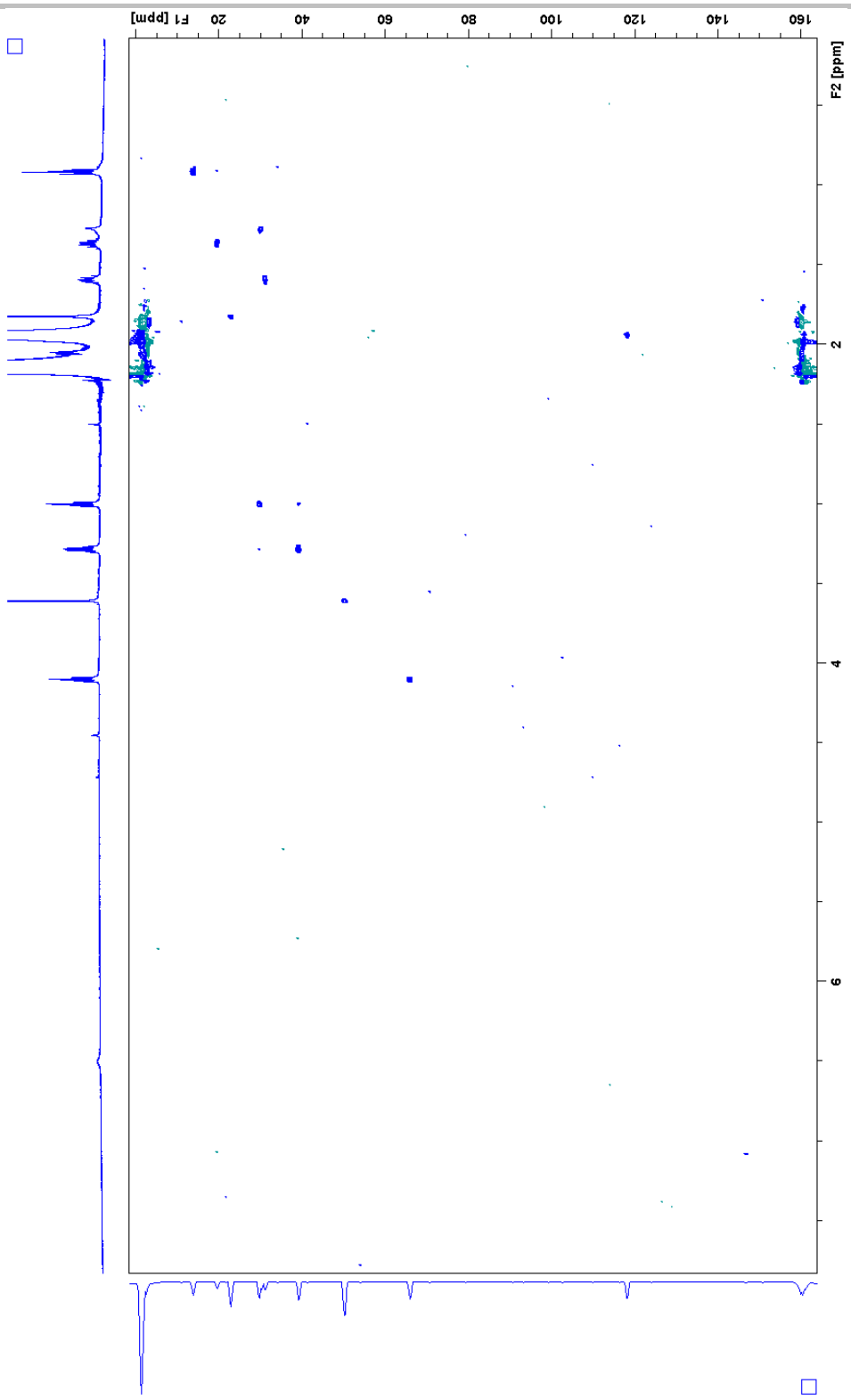

Figure S12: HSQC spectrum of **18** in acetonitrile-d_3.

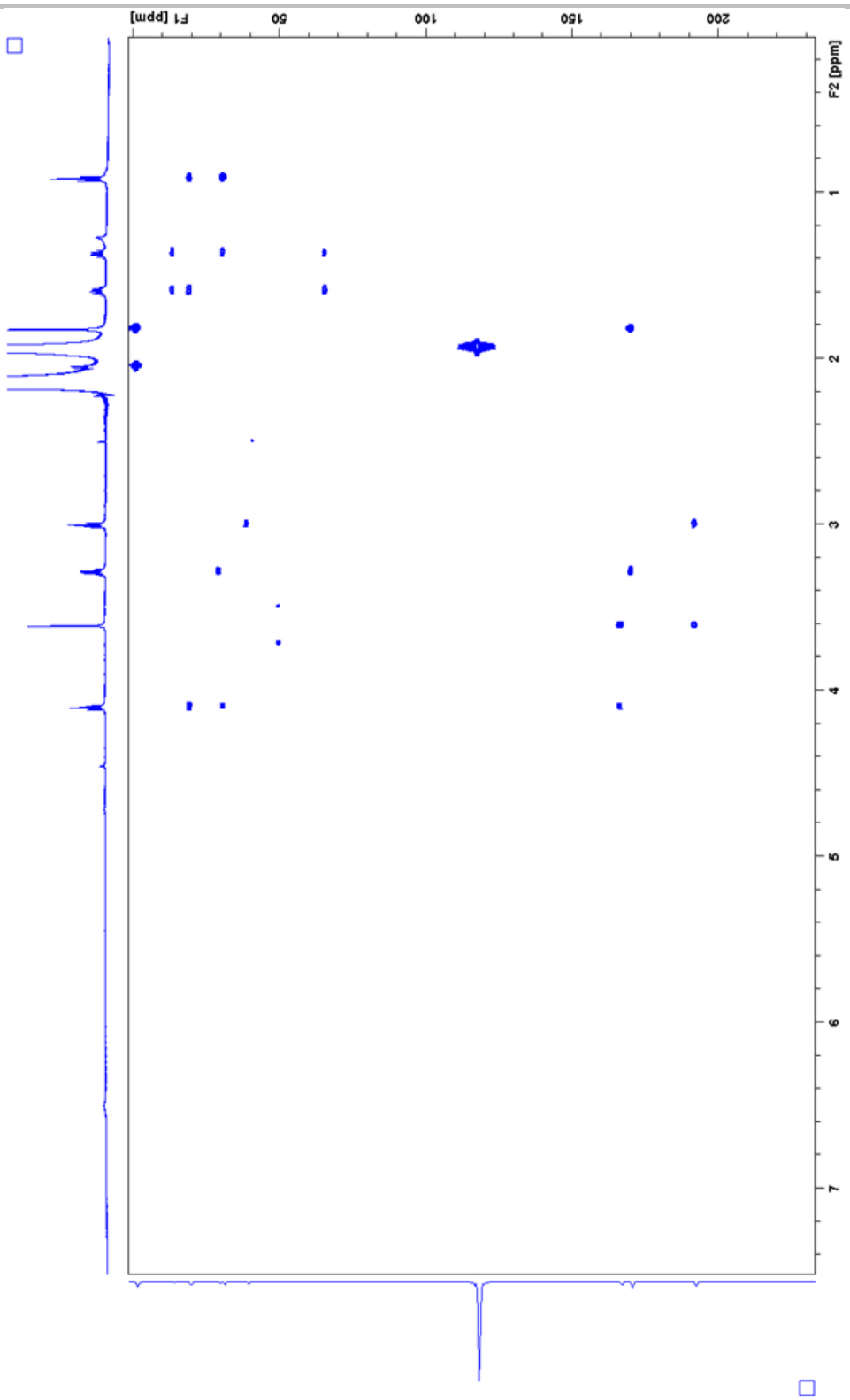

Figure S13: HMBC spectrum of **18** in acetonitrile-d_3.

A

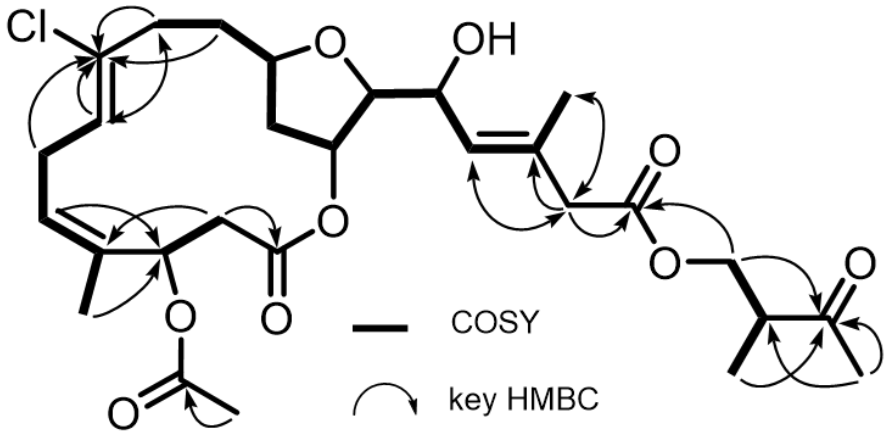

B

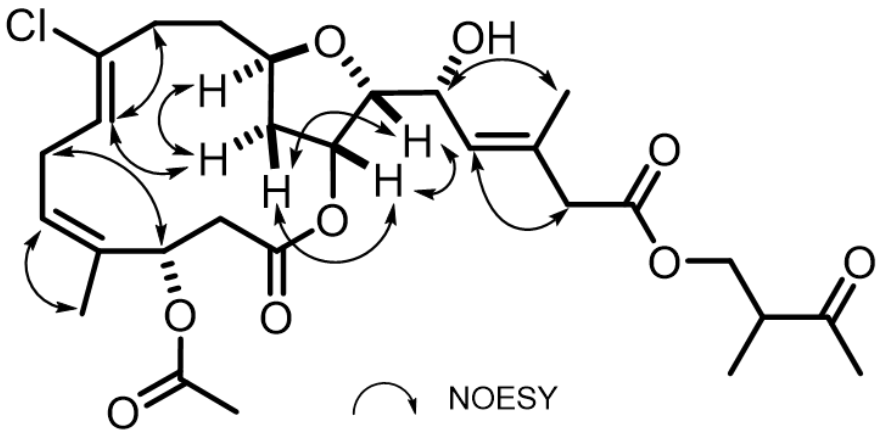

Figure S14: Key correlations of oocydin B (**24**). (*A*) COSY and key HMBC correlations of oocydin B. (*B*) Key NOESY correlations of oocydin B with deduced relative stereochemistry.

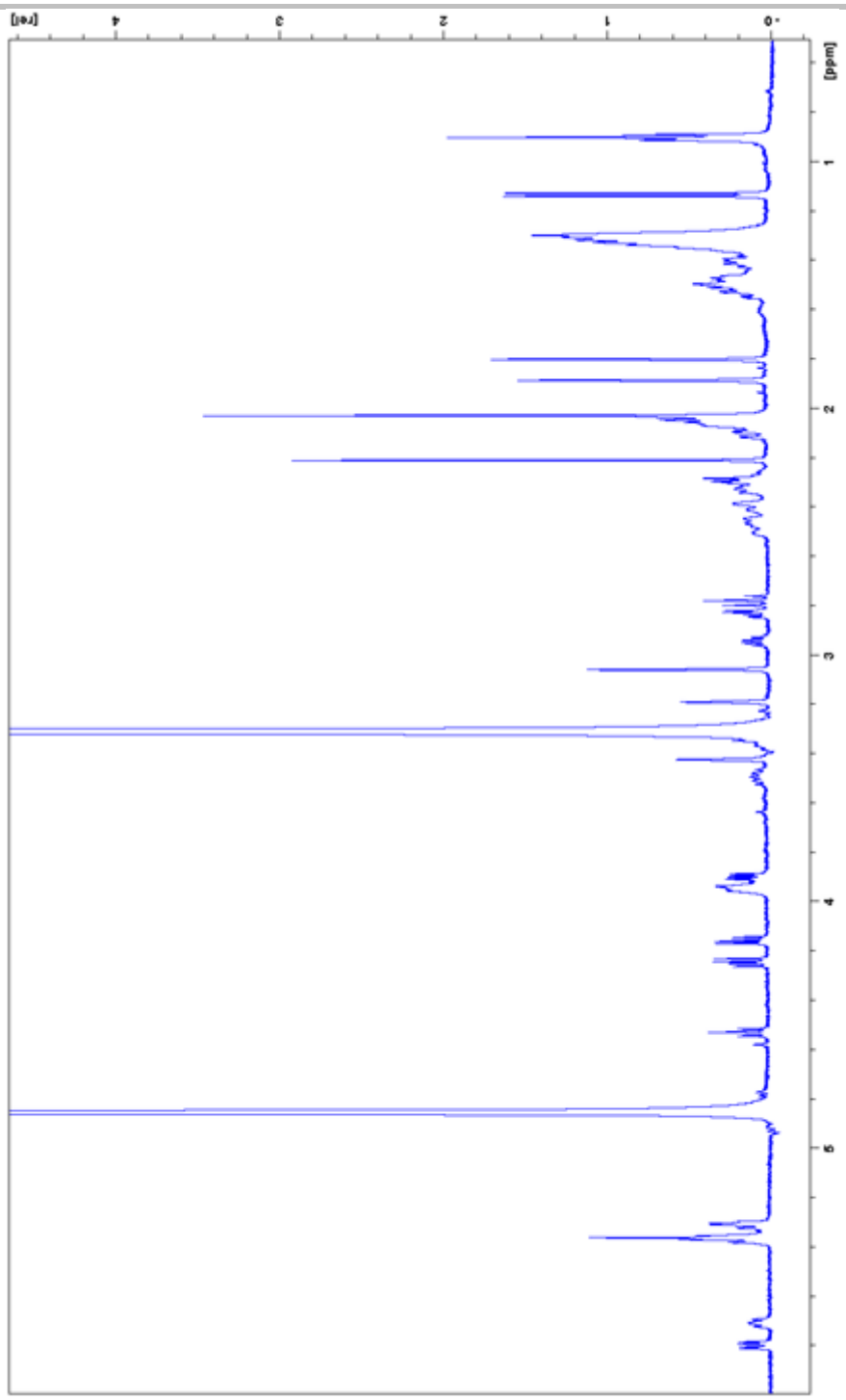

Figure S15: ^{1}H NMR spectrum of oocydin B (**24**) in methanol-d_4 at 600 MHz.

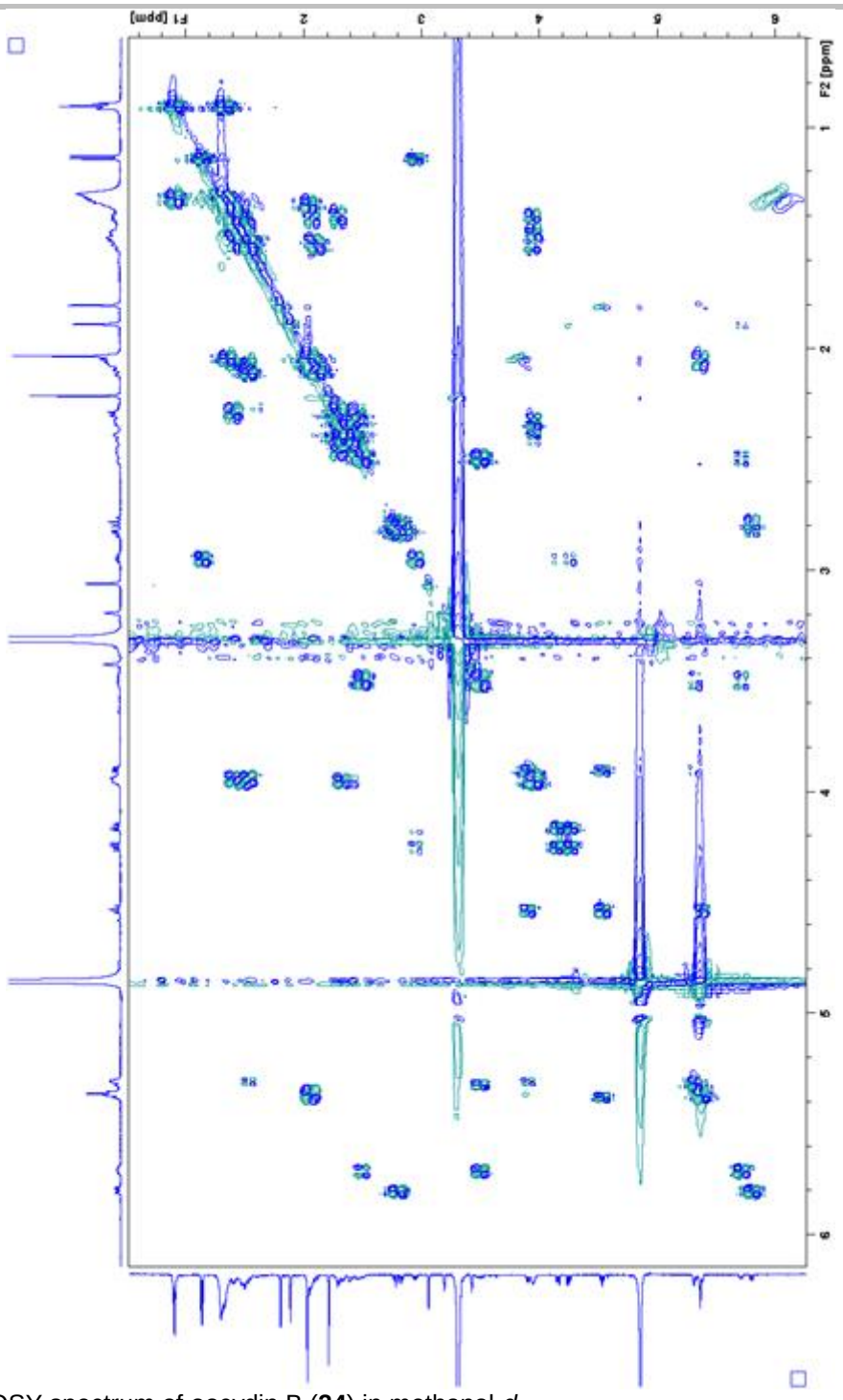

Figure S16: COSY spectrum of oocydin B (**24**) in methanol-d_4.

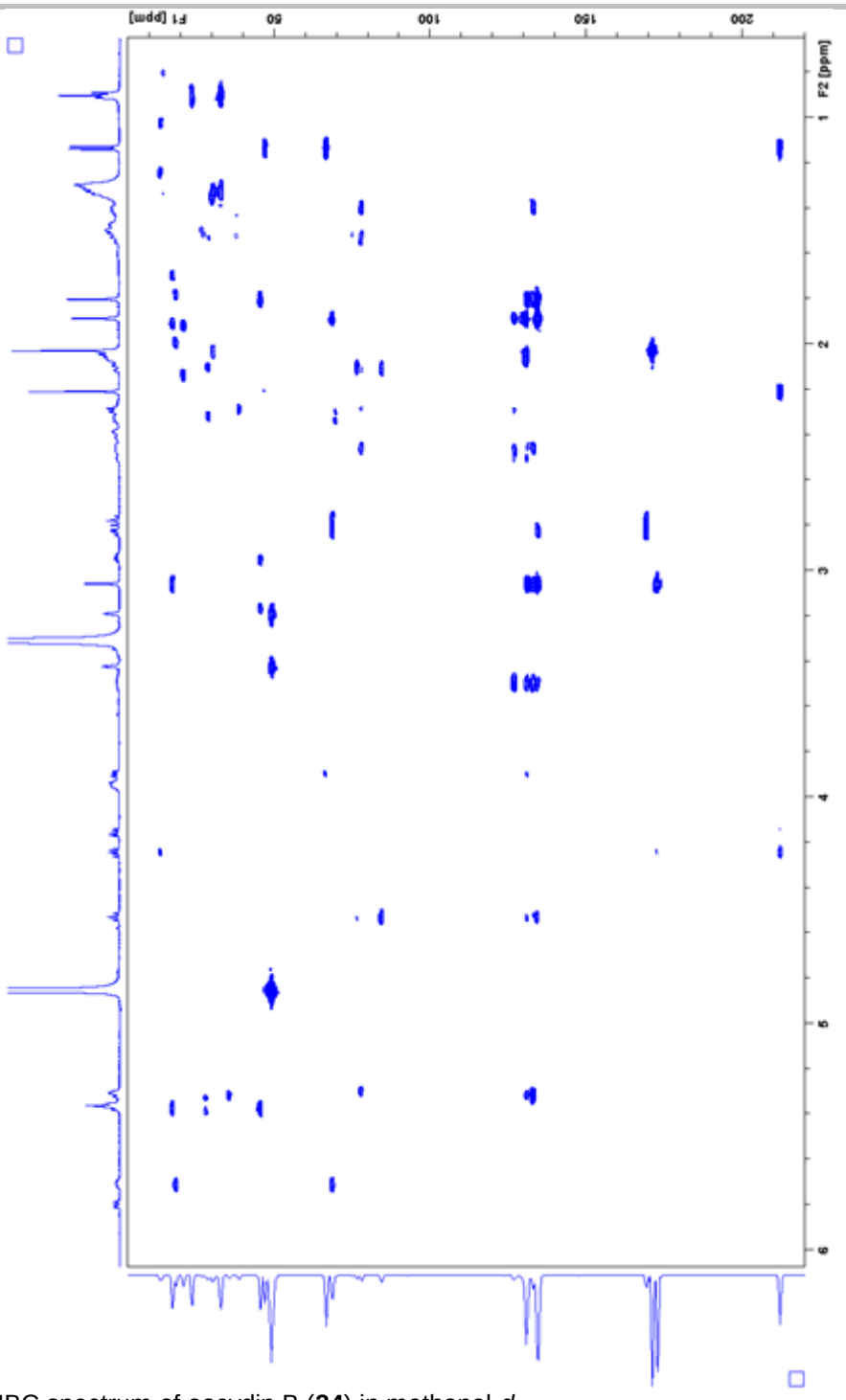

Figure S17: HMBC spectrum of oocydin B (**24**) in methanol-d_4.

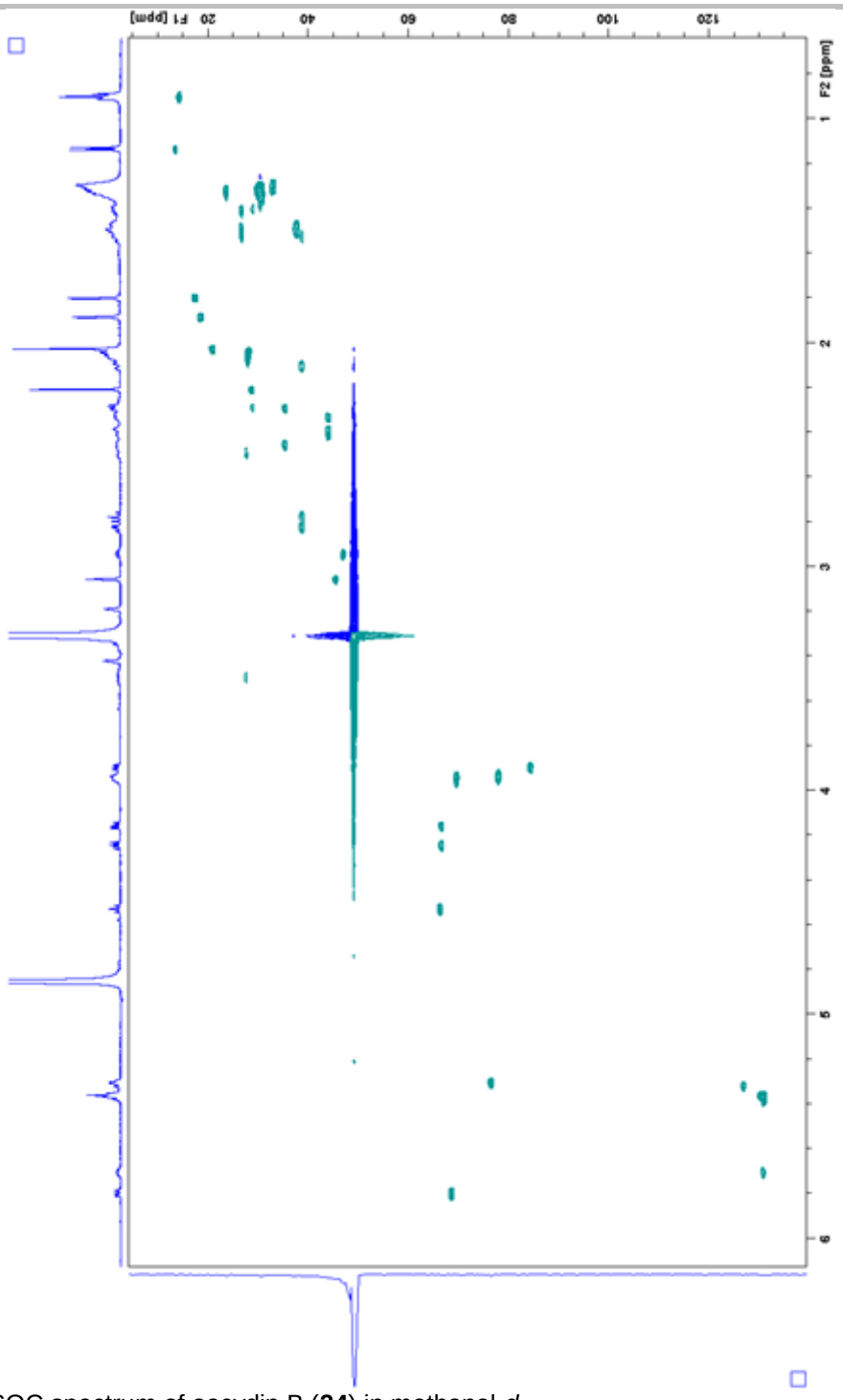

Figure S18: HSQC spectrum of oocydin B (**24**) in methanol-d_4.

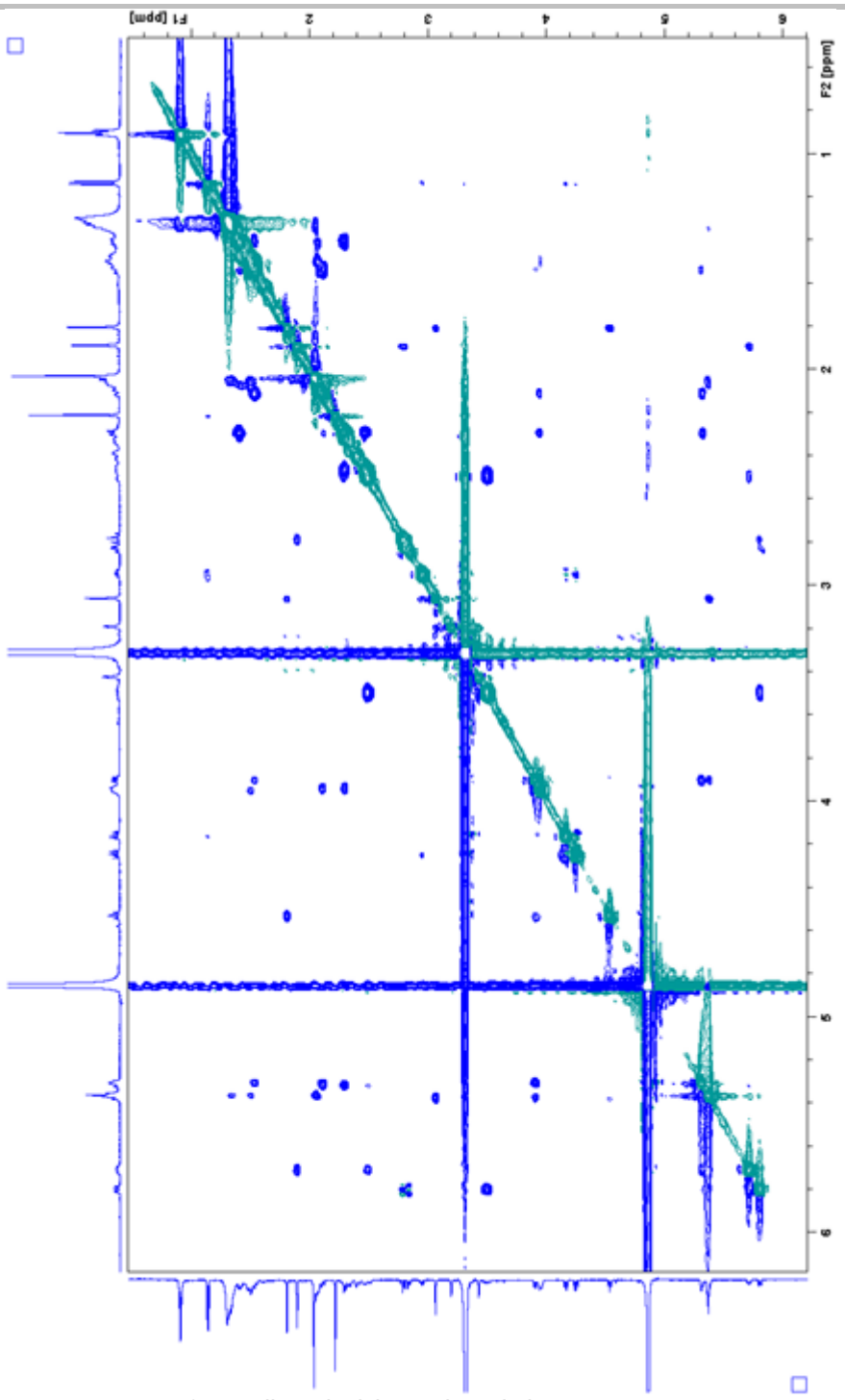

Figure S19: NOESY spectrum of oocydin B (**24**) in methanol-d_4.

SUPPORTING INFORMATION

Table S1. Primers used in this work.

Primer Name	Primer Sequence
*oocKNco*I_F	CTAGCCATGGATGGATGTACAAGG
*oocKBgl*II_R	GCAGATCTCTACCTTCTATTGAGTAC
pBAD*oocKNde*IQC_F	GAATTAACCACATATGGATGTACAAGGAAAACGAGTATG
pBAD*oocKNde*IQC_R	CCATATGTGGTTAATTCCTCCTGTTAGCCCAAAAAAC
*oocK*N'*Not*I_R	CATGCGGCCGCCTACCTTCTATTGAGTAC
*pedGPci*I_F	CGACATGTATGAATCAGAAATTTAGATTATGC
*pedGHind*III_*R*	GGTAAGCTTTCAGATTTCATCCAGCATTTC
pBAD*pedGNde*IQC_F	GGAATTAACCACATATGAATCAGAAATTTAGATTATGC
pBAD*pedGNde*IQC_R	TTCATATGTGGTTAATTCCTCCTGTTAGCCCAAAAAAC
*tobDNco*I_F	CTAGCCATGGATGAGGCAGGAACGGATC
*tobDHind*III_R	GCTCTAAGCTTGATCATTGCCGGAGCTTCG
pBAD*tobDNde*IQC_F	GGAATTAACCACATATGAGGCAGGAACGGATCGGAATC
pBAD*tobDNde*IQC_R	CCTCATATGTGGTTAATTCCTCCTGTTAGCCCAAAAAAC
KO_SOD_b00960_fwd	GCGTATGGAATGCTGACAGCCGCTGTGGCCGCACCTATCCGTCATTGCATAATTAACCCTCACTAAAGGGCGG
KO_SOD_b00960_rev	TAATGAGGATAATCTTCCGGCATGGGGAAATCCGGATATTGGGTATTGACTAATACGACTCAC TATAGGGCTC

Table S2. NMR data for **18** measured in acetonitrile-d_3.

No.	δ_C	δ_H, mult.
1	192.5	
2	50.3	3.61 s
3	167.0	
4	29.5	3.00 (t, 6.5)
5	31.2	1.57-1.62 m
6	19.5	1.34-1.40 m
7	13.8	0.92 (t, 7.4)
8	39.2	3.27-3.31 m
9	66.0	4.10 (t, 6.6)
9-NH		6.50 brs
10	170.7	
11	22.8	1.83 s

Table S3. NMR data for **24** measured in MeOH-d_4.

No.	δ_C	δ_H, mult.
1	169.3	
2	38.8	2.78 (dd, 11.5, 11.5)
		2.83 (dd, 4.5, 11.5)
3	68.7	5.80 (dd, 4.5, 11.5)
4	134.6	
5	130.8	5.71 m
6	27.6	2.49 m
		3.49 m
7	127.0	5.32 ovlp.
8	133.0	
9	35.3	2.29 ovlp.
		2.46 m
10	28.9	1.40 ovlp.
		2.29 ovlp.
11	78.0	3.94 ovlp.
12	38.7	1.53 ovlp.
		2.11 (dd, 3.1, 13.3)
13	76.5	5.31 ovlp.
14	84.4	3.90 (dd, 3.7, 8.7)
15	66.3	4.53 (dd, 8.7, 8.7)
16	130.9	5.38 ovlp.
17	134.4	
18	45.6	3.06 s
19	172.9	
20	171.2	
21	20.9	2.03 s
22	18.5	1.89 brs
23	17.3	1.80 brd
24	66.6	4.16 (dd, 5.4, 11.2)
		4.25 (dd, 7.2, 11.2)
25	47.0	2.95 m
26	212.2	
27	28.7	2.21 s
28	13.5	1.14 (d, 7.2)

References

[1] E. J. Helfrich, J. Piel, *Nat. Prod. Rep.* **2016**, *33*, 231-316.
[2] R. C. Edgar, *Nucleic Acids Res.* **2004**, *32*, 1792-1797.
[3] K. Tamura, G. Stecher, D. Peterson, A. Filipski, S. Kumar, *Mol. Biol. Evol.* **2013**, *30*, 2725-2729.
[4] I. Letunic, P. Bork, *Bioinformatics* **2006**, *23*, 127-128.
[5] a) J. Lopera, I. J. Miller, K. L. McPhail, J. C. Kwan, *mSystems* **2017**, *2*, e00096-00017; b) T. Wakimoto, Y. Egami, Y. Nakashima, Y. Wakimoto, T. Mori, T. Awakawa, T. Ito, H. Kenmoku, Y. Asakawa, J. Piel, I. Abe, *Nat. Chem. Biol.* **2014**, *10*, 648-655.
[6] C. R. Huitt-Roehl, E. A. Hill, M. M. Adams, A. L. Vagstad, J. W. Li, C. A. Townsend, *ACS Chem. Biol.* **2015**, *10*, 1443-1449.
[7] I. Koryakina, J. B. McArthur, M. M. Draelos, G. J. Williams, *Org. Biomol. Chem.* **2013**, *11*, 4449-4458.
[8] M. Jenner, S. Frank, A. Kampa, C. Kohlhaas, P. Pöplau, G. S. Briggs, J. Piel, N. J. Oldham, *Angew. Chem. Int. Ed.* **2013**, *52*, 1143-1147.
[9] S. Grüschow, T. J. Buchholz, W. Seufert, J. S. Dordick, D. H. Sherman, *ChemBioChem* **2007**, *8*, 863-868.
[10] C. Kohlhaas, M. Jenner, A. Kampa, G. S. Briggs, J. P. Afonso, J. Piel, N. J. Oldham, *Chemical Science* **2013**, *4*, 3212-3217.
[11] T. Mori, J. K. B. Cahn, M. C. Wilson, R. A. Meoded, V. Wiebach, A. F. C. Martinez, E. J. N. Helfrich, A. Albersmeier, D. Wibberg, S. Dätwyler, R. Keren, A. Lavy, C. Rückert, M. Ilan, J. Kalinowski, S. Matsunaga, H. Takeyama, J. Piel, *Proc. Natl. Acad. Sci. U. S. A.* **2018**.
[12] S. Frank, Universitäts-und Landesbibliothek Bonn **2014**.
[13] J. Piel, *Proc. Natl. Acad. Sci. U. S. A.* **2002**, *99*, 14002-14007.
[14] D. Domik, A. Thürmer, T. Weise, W. Brandt, R. Daniel, B. Piechulla, *Frontiers in microbiology* **2016**, *7*, 737.
[15] M. Wang, J. J. Carver, V. V. Phelan, L. M. Sanchez, N. Garg, Y. Peng, D. D. Nguyen, J. Watrous, C. A. Kapono, T. Luzzatto-Knaan, C. Porto, A. Bouslimani, A. V. Melnik, M. J. Meehan, W. T. Liu, M. Crüsemann, P. D. Boudreau, E. Esquenazi, M. Sandoval-Calderon, R. D. Kersten, L. A. Pace, R. A. Quinn, K. R. Duncan, C. C. Hsu, D. J. Floros, R. G. Gavilan, K. Kleigrewe, T. Northen, R. J. Dutton, D. Parrot, E. E. Carlson, B. Aigle, C. F. Michelsen, L. Jelsbak, C. Sohlenkamp, P. Pevzner, A. Edlund, J. McLean, J. Piel, B. T. Murphy, L. Gerwick, C. C. Liaw, Y. L. Yang, H. U. Humpf, M. Maansson, R. A. Keyzers, A. C. Sims, A. R. Johnson, A. M. Sidebottom, B. E. Sedio, A. Klitgaard, C. B. Larson, P. C. Boya, D. Torres-Mendoza, D. J. Gonzalez, D. B. Silva, L. M. Marques, D. P. Demarque, E. Pociute, E. C. O'Neill, E. Briand, E. J. Helfrich, E. A. Granatosky, E. Glukhov, F. Ryffel, H. Houson, H. Mohimani, J. J. Kharbush, Y. Zeng, J. A. Vorholt, K. L. Kurita, P. Charusanti, K. L. McPhail, K. F. Nielsen, L. Vuong, M. Elfeki, M. F. Traxler, N. Engene, N. Koyama, O. B. Vining, R. Baric, R. R. Silva, S. J. Mascuch, S. Tomasi, S. Jenkins, V. Macherla, T. Hoffman, V. Agarwal, P. G. Williams, J. Dai, R. Neupane, J. Gurr, A. M. Rodriguez, A. Lamsa, C. Zhang, K. Dorrestein, B. M. Duggan, J. Almaliti, P. M. Allard, P. Phapale, et al., *Nat. Biotechnol.* **2016**, *34*, 828-837.
[16] P. Shannon, A. Markiel, O. Ozier, N. S. Baliga, J. T. Wang, D. Ramage, N. Amin, B. Schwikowski, T. Ideker, *Genome Res.* **2003**, *13*, 2498-2504.

Author Contributions

RAM and JP designed the research and wrote the manuscript; RAM and EJNH performed the bioinformatic analyses; RAM and RU, did structural elucidation; RAM did the enzyme work; KJ isolated oocydin B; NM and BP generated *Serratia plymuthica* 4Rx13 knockout; RAM, RU and JP wrote the supporting information; RAM did the synthesis.